ARCHITECTURAL EFFECT ON MECHANICAL PROPERTIES OF 3D CARBON/PPS COMPOSITES

Joon-Hyung Byun, Yeun-Ho Yu, Kyeong-Sik Min, Jin-Woo Yi, Moon-Kwang Um
Korea Institute of Machinery & Materials

Keywords: *3-dimensional, thermoplastic, prepreg, mechanical property, impact, C-scan, damage*

Abstract

In order to fabricate the three-dimensional (3D) thermoplastic composites, the automated tape placement (ATP) process and a z-fiber insertion method have been utilized. The tape placement material for the ATP was carbon/epoxy prepreg tapes of 5mm width. Pultruded carbon/epoxy rods with nominal diameter of 1mm were used for the reinforcement in the thickness direction. Two-dimensional (2D) composites have also been fabricated to compare with 3D composites in terms of the mechanical properties and the low velocity impact damage tolerance. The tensile, compressive, and shear properties of 3D composites were reduced because of the decreased fiber volume fraction. However, the size of damage area of 3D samples was greatly reduced by 55%-70% due to the z-fibers. The residual strengths of 3D composites, according to compression-after-impact (CAI) tests, were less than those of 2D counterparts in general. This is due to that the smaller fiber volume fraction of 3D composites, and the local voids near the z-fibers.

1 Introduction

In the application of aircraft parts, polymer matrix composites such as carbon/epoxy laminates are dominant. However, they are liable to develop extensive damage under impact loading, eventually leading to delamination. The main reason for this is due to the brittle nature of epoxy materials and no reinforcements in the thickness direction of the laminated composites.[1-3] In order to overcome the shortcomings of conventional thermo-set laminated composites, several measures have been considered. [4,5] One of the feasible ways of delamination suppression is the use of thermoplastic materials. Although thermoplastics can enhance the ductility of composites, delamination suppression cannot be greatly improved in the laminated system because the fibers are reinforced only in the plane. The most effective way is by introducing through-thickness reinforcements in the fiber architecture. By utilizing the thermoplastic fibers and 3D textile process technology, we can obtain much higher damage tolerant composites.

3D textiles fabricated by braiding, weaving or stitching methods provide fully integrated continuous fiber orientations. The feasible type of material for textile processing is the commingled yarns. Another type of hybridized yarn, the co-braided yarn, for 3D textile performing has been recently introduced [6]. However, the production rate of 3D preforming is slow due to many fiber bundles interlacing several layers. The size of 3D perform is also limited and dependent on the capacity of textile machines.

Although utilization of hybrid yarns attracts much interest in the manufacturing of thermoplastic composites due to the possibility of complex shapes and cost-effective production, most composite parts in aerospace applications are manufactured with prepregs. The reason of preference for prepregs may be the familiarity, handing, property reliability, low voids, and high fiber volume fraction. However, it is not feasible to construct 3D fiber architectures using prepregs due to their stiff nature.

In this paper, we suggest a method of producing 3D composites by utilizing prepregs and a z-fiber insertion technique. The purpose of this study has two-folds: (1) manufacturing of 3D thermo-plastic composites; (2) characterization of 3D composites and comparison their mechanical properties with conventional prepreg tape laminates in order to find their potential application for aircraft parts.

2 Experimental

2.1 ATP Process

In order to introduce through-thickness fibers in the lay-ups of prepreg tapes, there should be

through-thickness holes. In this study, generation of holes are achieved by laying down prepreg tapes with a gap side by side, and by repeating this process layer by layer with different orientation. When the required thickness is obtained, the stacked prepregs have regularly-positioned holes, which will provide the penetration of through-thickness fibers. Terms in this paper are defined as: 'prepreg tape' refers to prepreg with certain width, and 'prepreg sheet' is the conventional prepreg. To lay down prepreg tapes with controlled gap, highly precise and automated machine is required. In this work, the automated tape placement (ATP) process has been utilized for stacking of prepreg tapes.

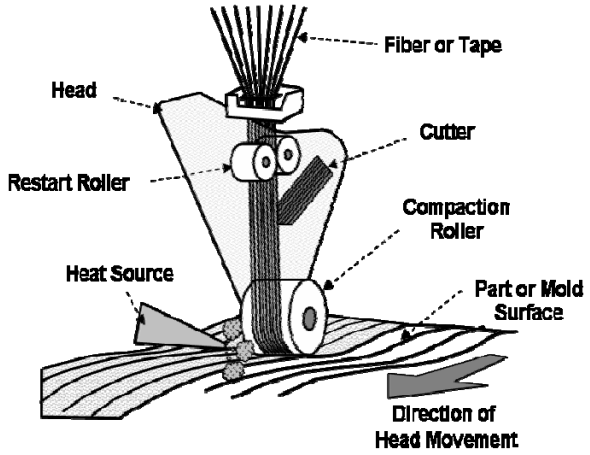

Fig. 1 Automated tape placement process.

Fig. 1 shows ATP process, explained as follows. Prepreg tapes are pulled off the spools and delivered into a fiber placement head. They are laid down and compacted onto a mold surface by a compaction roller, and are at the same time on-line consolidated by a heat source. At the end of the course, the remaining tows are cut and the head is positioned to the beginning of the next course. At the next course, restart rollers are activated, and tow placement (lay-down and consolidation) is repeated. The tape placement has been carried out by 6-axis controlled FPS (Fiber Placement System) machine as shown in Fig. 2.

2.2 Materials

The prepregs are carbon/PPS (Polyphenylene Sulfide), supplied from Phoenixx TPC. By DSC (Differential Scanning Calorimetry) test, the melting temperature, and the glass transition temperature of PPS were around 260°C and 98°C, respectively. For this type of prepreg, 1160P-150-12, carbon fibers were AS-4C, and fiber volume fraction was 58.3%. For the purpose of z-fiber insertion, carbon/PPS rods of nominal diameter of 1mm were utilized. They were pultruded by the same company. Fig. 3 shows the cross-section of the pultruded rod.

Fig. 2 Fiber placement system.

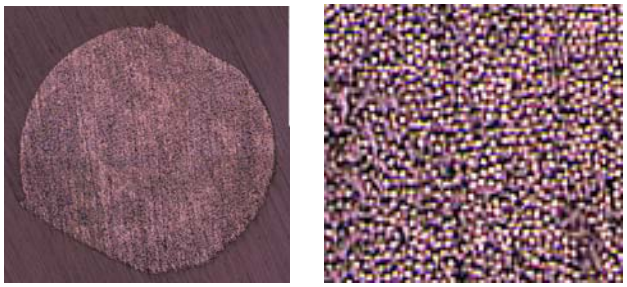

(a) (b)

Fig, 3 Cross-section of a carbon/PPS rod: (a) entire section; (b) fiber distribution.

2.3 Sample Preparation

For the comparison with 3D composites, orthogonal laminates, stacking sequence of [/0/90]ns, have been fabricated. In 3D composites, it is necessary for providing a space for the rod insertion. By laying-up the 5mm wide prepreg tapes in 0° and 90° with leaving small space (1mm), cross-ply laminates has been obtained. In the space of 1mm-square gaps in the whole through-thickness direction, carbon/PPS rods were inserted. Fig. 4 (a) shows the semi-consolidated sample after ATP process. Carbon/PPS rods were inserted by hands in the through-thickness gaps after it was taken out from

the FPS machine. Fig. 4 (b) shows the 3D sample after the rod insertion. In order to fill the empty spaces between prepreg tapes three layers of PPS films were added before the final consolidation. Fig. 5 shows the process cycle for the 2D and 3D composites fabrication.

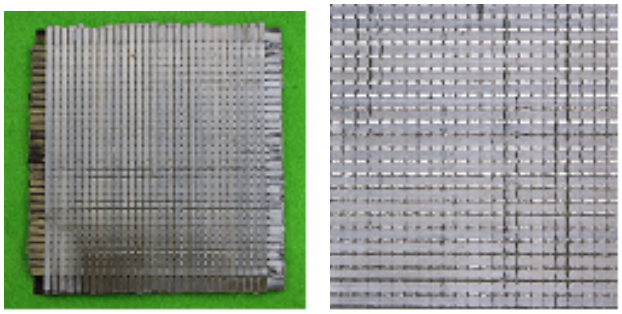

(a) (b)

Fig. 4 Fabrication of 3D composites: (a) semi-consolidated sample after ATP process; (b) composites after rod insertion.

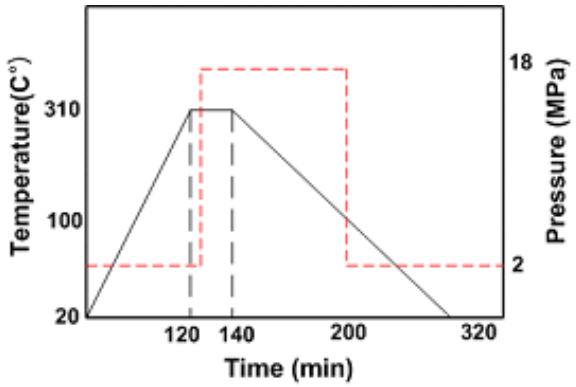

Fig. 5 Hot press processing cycle.

Fig. 6(a) shows the carbon/PPS rods on the cross-sections of 3D specimen. White area is the 0^o layers, and dark one corresponds to 90^o layers. Fig. 6 (b) is the longitudinal section which does not involve through-thickness rods. The straightness of 0^o layers demonstrates that overall placement of prepreg tapes by ATP process is excellent. Fig. 6 (c) is the section in the sample plane, which shows the deformed shape of carbon/PPS rods due to the interference of prepreg tapes on the plane.

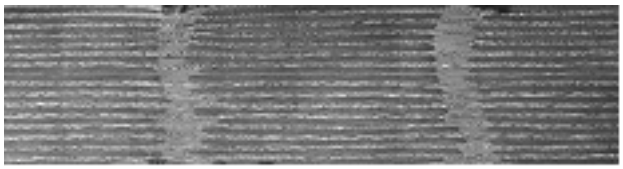

(a)

(b)

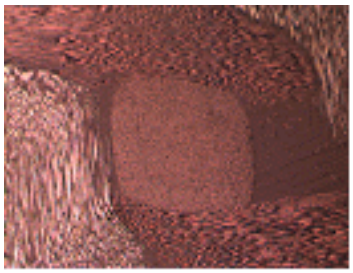

(c)

Fig. 6 Microstructures of 3D composites: (a) a section along the 0 fiber direction incorporated with carbon/PPS rods; (c) a section along the same direction without rods; (c) a section in the sample plane showing the cross-section of a rod..

3 Results

3.1 Mechanical Tests

To obtain strength and modulus of composites, specimens were tested under tension, compression, and shear loading based on ASTM D3039, ASTM D695, and ASTM D5379, respectively. Properties of unidirectional composites (V_f = 53%) were summarized in Table 1.

Table 2 summarizes the basic property results of orthogonal and 3D composites. The strength and Young's modulus of 3D specimen were less than those of 2D samples. This is because the fiber volume fraction of 3D specimen (V_f = 47.1%) is smaller than that of the counterpart (V_f = 52.7%). The fiber content of 3D specimen is less due to the space for the carbon/PPS rod insertion. However, the existence of through-thickness rods gave higher shear strength of 3D specimen.

Figs 7 (a) and (b) show the comparison of strength and modulus between 2D and 3D composites. The tensile and compressive strengths of 3D specimen were reduced by 7% and 12%, but shear strength increased by 36%. The tensile, compressive, and shear moduli were decreased by 6%, 16%, and 18%, respectively.

Table 1 Basic property of UD carbon/PPS

Property			Average (SD)
Tensile	0°	Strength (((MPa)	1459 (±12.6)
		Modulus (GPa)	107.0 (±9.92)
	90°	Strength (MPa)	59.6 (±8.99)
		Modulus (GPa)	9.93 (±0.20)
Compres-sion	0°	Strength (MPa)	1148 (±97.8)
		Modulus (GPa)	109.9 (±5.11)
	90°	Strength (MPa)	122.4 (±17.0)
		Modulus (GPa)	8.91 (±0.38)
Shear		Strength (MPa)	67.7 (±1.36)
		Modulus (GPa)	5.12 (±0.22)

Table 2 Basic properties of orthogonal and 3D composites

Property			Average (SD)
Tensile	2D	Strength (MPa)	706 (±83.5)
		Modulus (GPa)	63.7 (±6.04)
	3D	Strength (MPa)	655 (±73.9)
		Modulus (GPa)	59.5 (±2.85)
Compres-sion	2D	Strength (MPa)	582 (±29.5)
		Modulus (GPa)	57.9 (±8.62)
	3D	Strength (MPa)	511 (±66.7)
		Modulus (GPa)	49.6 (2.84)
Shear	2D	Strength (MPa)	125.1 (±19.4)
		Modulus (GPa)	4.25 (0.51)
	3D	Strength (MPa)	171.2 (±45.3)
		Modulus (GPa)	3.47 (±0.18)

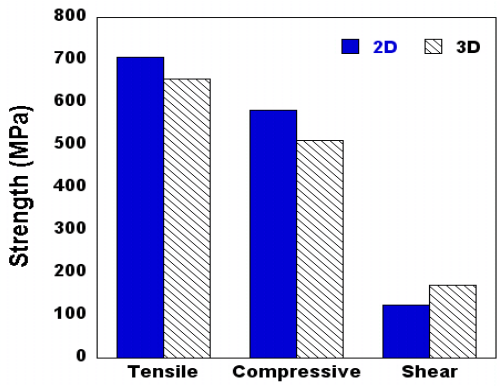

(a)

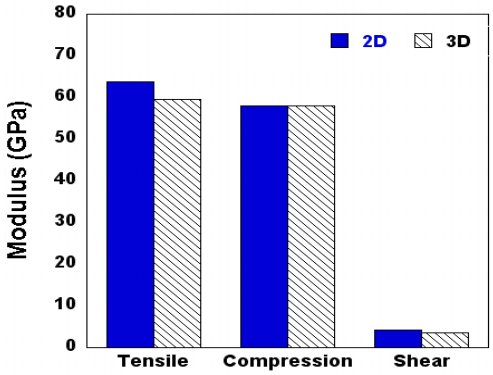

(b)

Fig. 7 Comparison of elastic properties of 2D and 3D composites: (a) strength; (b) modulus.

3.2 Low Velocity Impact Test

To examine the damage resistance of the 3D composites the low velocity drop weight impact test has been adopted. For the comparison of impact performance, 2D laminates were also tested. The energy levels imposed to the specimens were controlled by adjusting the height of the impactor which weighs 7.96 kg with a hemisphere's diameter of 15.88 mm. The impact energy levels were 20J, 25J, 30J, and 35J [7]. The specimen size was 150 x 100 mm according to SACMA SRM 2R-94 test specification. For the assessment of damage after impact loading, specimens were subjected to C-scan non-destructive inspection. CAI test was conducted to evaluate residual compressive strength of the impacted specimen.

Figure 8 (a) and (b) show the load-time histories for 2D and 3D composites. For the highest energy level of 35J, 2D composites showed drastic load drop of 3000N level and the maximum load is 10000N, approximately. 3D composites, however, resulted in a small amount of load drop, and the maximum load was around 7000N. The large amount of load drop in 2D composites is due to that most of impact energy was absorbed in the form of delamination. In 3D composites, however, impact energy was absorbed in creating delamination and crack propagation in the through-thickness rods. The results of load-displacement in Fig. 9 (a) showed that the magnitude of permanent deformation for 2D composites was nearly the same for all the energy levels. However, the deformation of 3D composites is proportional to the energy levels as shown in Fig. 9 (b). This clearly indicates that delamination is the major mode of failure for the case of 2D composites, while in 3D composites, delamination is suppressed

by through-thickness fibers and a large deformation occurred due to the less fiber content. The absorbed impact energy, which is the enclosed area of the load-displacement curve, of 3D composites is much higher than that of the 2D counterpart.

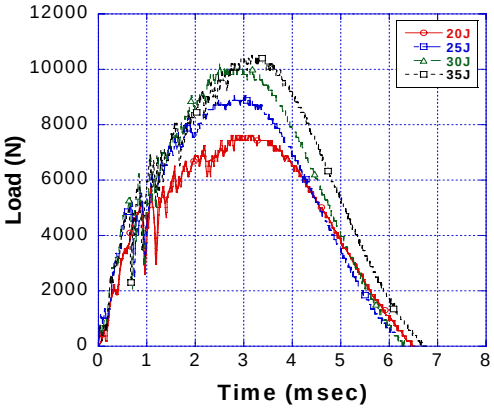

(a)

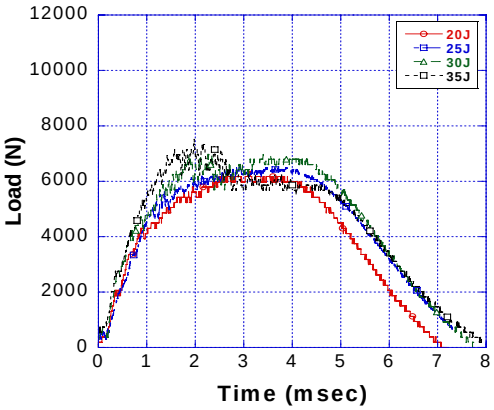

(b)

Fig. 8 Load-time curves: (a) 2D composite; (b) 3D composite.

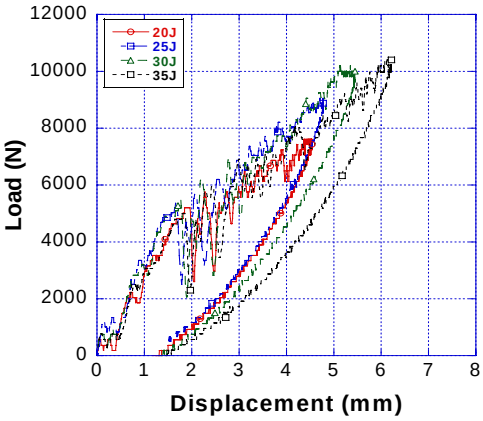

(a)

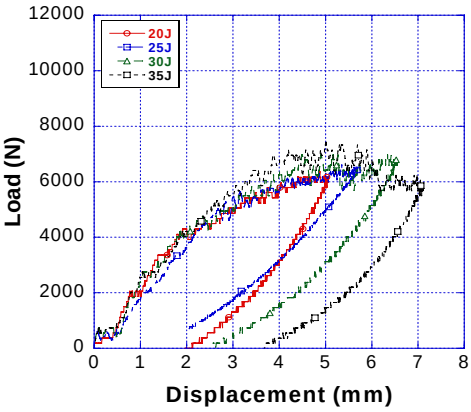

(b)

Fig. 9 Load-displacement curves: (a) 2D composites; (b) 3D composites.

Fig. 10 is C-scan images for impact energy of 20J, 25J, 30J and 35J. The damage areas indicate the pile-up images of the damage in the thickness direction. Cross stripes shown in 3D composites are the resin area formed at the gaps between prepreg tapes, which is due to the acoustic impedance difference of resins from the neighboring composites. The results of C-scan image clearly demonstrate that damage area of 3D specimen is smaller than that of 2D counterpart.

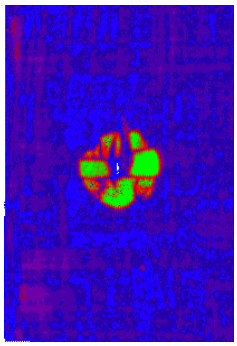

(a) 2D, 20J

(b) 3D, 20J

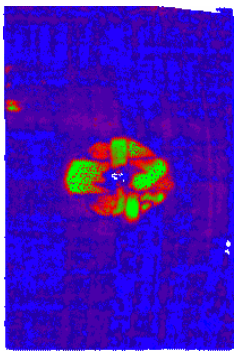

(c) 2D, 25J

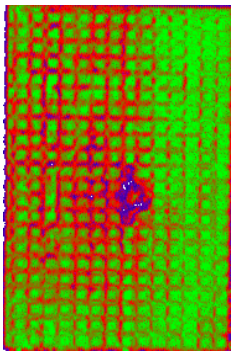

(d) 3D, 25J

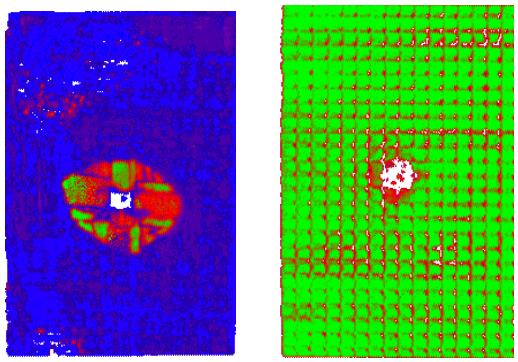

(e) 2D, 30J (f) 3D, 30J

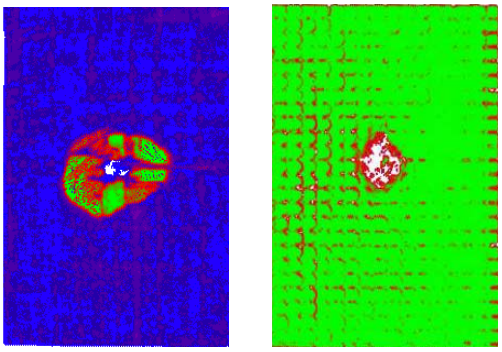

(g) 2D, 35J (h) 3D, 35J

Fig. 10 S-scan images of impacted area for 2D and 3D composites under various impact energies.

In order to facilitate the compressive failure in the damage area, four sides of impacted specimens were cut, which resulted in the specimen size of 70 mm x 105 mm for CAI tests. Table 3 summarizes the results of the impact test, C-scan, and CAI strength of 2D and 3D composites. Damage area of 3D composites was smaller than that of 2D composites. In each energy level, the damage area of 3D composites reduced by 55% - 70%.

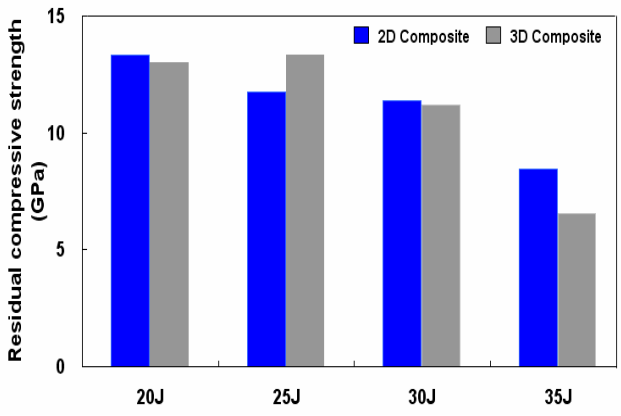

Fig. 11 CAI test results.

Fig. 11 shows the comparison of CAI strength of 2D and 3D composites for the tested energy levels. As the energy level increases the residual compressive strength of 2D samples decreases. However, in 3D composites, the residual strength of 25J was higher than 20J. Observation of 3D samples after compression test revealed that in some specimens, kink lines started at the site other than the impact damage area. The gaps for the z-fiber insertion, and the local voids near the z-fibers due to the lack of resin can be the possible reason for the inconsistent trend for 3D composites.

The residual strengths of 3D composites were less than those of 2D counterparts in general. This is due to that the smaller fiber volume fraction of 3D composites, and the local voids near the z-fibers. Nevertheless, the residual strengths of 3D composites are not greatly reduced than those of 2D samples. This is because delamination growth is limited due to the existence of z-fibers. In order to fully evaluate the performance of 3D composites, it is necessary to further research on the consolidation processing of 3D composites with full impregnations at z-fiber insertion areas.

Table 3 Impact test results of 2D and 3D composites

Material types	Properties				
	Thickness	Impact energy/ thickness, [J/mm]	Impact energy loss/ thickness, [J/mm]	Damage area [mm^2]	Residual compressive strength [GPa]
2D Composite	4.603	4.38	2.35	571 (±33.1)	13.31 (±0.85)
	4.959	4.93	2.72	681 (±153)	11.74 (±1.478)
	4.748	6.41	3.31	1292 (±54.1)	11.37 (±1.793)
	4.585	7.74	3.97	1831 (±249)	8.47 (±0.71)
3D Composite	4.9	4.07	61.2	195.7 (±31.8)	13.01 (±3.87)
	4.295	5.74	58.13	291 (±42.9)	13.31 (±1.992)
	4.838	6.28	70.9	402 (±42.3)	11.21 (±2.41)
	5.117	6.92	75.9	594 (±65.1)	6.53 (±0.61)

Fig. 12 shows the average of damage area divided by impact energy per unit thickness. Since this graph demonstrates the damage area per unit energy, regardless of the magnitude of impact energy, impact performance of composite materials can be compared directly. The length scale is the standard deviation. From this figure, 3D specimens have smaller damage area than 2D counterpart.

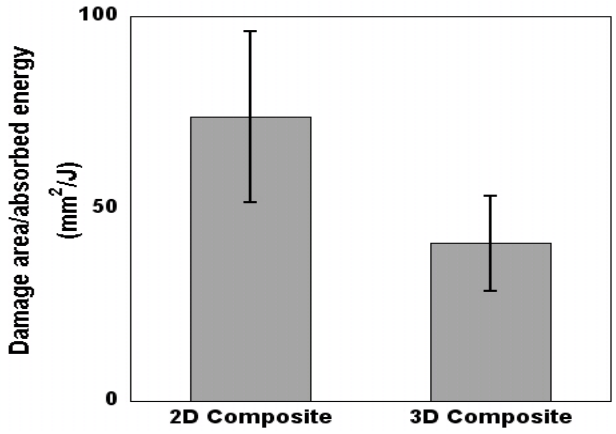

Fig. 12 Comparison of damage area per absorbed energy.

4 Conclusions

(1) The 3D composites were successfully fabricated by utilizing an automated tape placement process and the rod insertion technique. The carbon/PPS prepreg tapes of 5mm wide were used in the 0/90 placement, then pultruded rods of the same material were inserted through the 1mm x 1mm gaps in the thickness direction. The 3D textile composite panels of 200mm×300mm have been manufactured by compression molding process. Examining of composite microstructures demonstrated the uniform fiber distribution and complete infiltration of PPS matrix. The fiber volume fraction of the sample was 47%.

(2) Compared with 2D cross-ply laminated composites, the tensile and compressive strengths of 3D specimen were reduced by 7% and 12%, but shear strength increased by 36%. The tensile, compressive, and shear moduli were decreased by 6%, 16%, and 18%, respectively. The reason for this is due to the smaller fiber volume fraction of 3D composites.

(3) For 20J, 25J, 30J, and 35J of impact energy, the damage area of 3D specimen was smaller than that of 2D specimen. In each energy level, the damage area of 3D composites reduced by 55% - 70%. The residual strengths of 3D composites were less than those of 2D counterparts in general. This is due to that the smaller fiber volume fraction of 3D composites, and the local voids near the z-fibers. Nevertheless, the residual strengths of 3D composites are not greatly reduced than those of 2D samples.

(4) In order to fully evaluate the performance of 3D composites, it is necessary to further research on the consolidation processing of 3D composites with full impregnations at z-fiber insertion areas.

Acknowledgement

This research was supported by a grant from the National Research Laboratory funded by the Ministry of Science and Technology, Republic of Korea.

References

[1] Abrate, S., *Impact on composite structures*, Cambridge: Cambridge University Press, 1998.

[2] Schoeppner, G.A. and Abrate, S., "Delamination threshold loads for low velocity impact on composite laminates," *Composites Part A*, Vol. 31, 2000, pp. 903-915.

[3] Mouritz, A.P., Leong K.H., and Herszberg, I., "A review of the effect of stitching on the in-plane mechanical properties of fibre-reinforced polymer composites," *Composites Part A*, Vol. 28 1997, pp. 979-991.

[4] Byun, J-H. and Chou, T-W., "Mechanics of Textile Composites," *Comprehensive Composite Material*, A. Kelly and C. Zweben (Eds), Elsevier Science Publishers, Amsterdam, Netherlands, Vol. 1, Chapter 22, 2000, pp. 719-761.

[5] Byun, J-H., Um, M-K., Hwang B-S., and Song S-W., "Impact Performance of 3D Interlock Textile Composites," Proceedings of the 4th Asian-Australasian Conference on Composite Materials (ACCM-4), Univ. of Sydney, Australia, July 6-9, 2004, pp. 488-493.

[6] Byun JH, Hong SG, Lee JH, Kang BS. "Process and Characterization of 3D Woven Carbon/PEEK Thermoplastic Composites," SAMPE-2006, Long Beach, CA, USA; April 30 - May 4, 2006.

[7] SACMA Recommended Test Method for CAI Properties of Oriented Fiber-Resin Composites: SRM 2R-94.